

BMB Reports – Manuscript Submission

Manuscript Draft

Manuscript Number: BMB-19-093

Title: Sinapic acid induces the expression of thermogenic signature genes and lipolysis through activation of PKA/CREB signaling in brown adipocytes

Article Type: Article

Keywords: Sinapic acid; Thermogenesis; Brown adipose tissue; Ucp1; PKA

Corresponding Author: Yong-Sik Kim

Authors: Monir Hossain^{1,2,#}, Khan Md. Imran^{1,2,#}, Md. Shamim Rahman^{1,2}, Dahyeon Yoon^{1,2}, Vignesh Marimuthu^{1,2}, Yong-Sik Kim^{1,2,*}

Institution: ¹Microbiology and ²Institute of Tissue Regeneration, College of Medicine, Soonchunhyang University,

1 **Manuscript Type:** Article

2 **Sinapic acid induces the expression of thermogenic signature genes and lipolysis through**
3 **activation of PKA/CREB signaling in brown adipocytes**

4
5 Monir Hossain^{1,2, †}, Khan Mohammad Imran^{1,2, †}, MD. Shamim Rahman^{1,2}, Dahyeon Yoon^{1,2},
6 Vignesh Marimuthu^{1,2} and Yong-Sik Kim^{1,2, *}

7 1: Institute of tissue regeneration, College of Medicine, Soonchunhyang University

8 2: Department of Microbiology, College of Medicine, Soonchunhyang University

9 **Running Tittle:** Sinapic acid induces the expression of thermogenic genes in brown adipocytes

10 **Keywords:** Sinapic acid, Brown adipocyte, UCP1, PKA, Browning, Lipolysis

11

12 †: Equal contribution

13 * Corresponding author: Yong-Sik Kim, Ph.D.

14 Department of Microbiology, College of Medicine

15 Soonchunhyang University

16 Soonchunhyang 6 gil 31, Dongnam-Gu, Cheonan, Chung-nam, 31151, Republic of Korea

17 Tel: +82-41-570-2413

18 Fax: +82-41-575-2412

19 Email: yongsikkim@sch.ac.kr

20 **ABSTRACT**

21 Lipid accumulation in white adipose tissue is the key contributor to the obesity and orchestrates
22 numerous metabolic health problems such as type 2 diabetes, hypertension, atherosclerosis, and
23 cancer. Nonetheless, the prevention and treatment of obesity are still inadequate. Recently,
24 scientists found that brown adipose tissue (BAT) in adult humans has functions that are
25 diametrically opposite to those of white adipose tissue and that BAT holds promise for a new
26 strategy to counteract obesity. In this study, we evaluated the potential of sinapic acid (SA) to
27 promote the thermogenic program and lipolysis in BAT. SA treatment of brown adipocytes
28 induced the expression of brown-adipocyte activation–related genes such as *Ucp1*, *Pgc1 α* , and
29 *Prdm16*. Furthermore, structural analysis and western blot revealed that SA upregulates protein
30 kinase A (PKA) phosphorylation with competitive inhibition by a pan-PKA inhibitor, H89. SA
31 binds to the adenosine triphosphate (ATP) site on the PKA catalytic subunit where H89 binds
32 specifically. PKA-cat- α 1 gene–silencing experiments confirmed that SA activates the thermogenic
33 program via a mechanism involving PKA and cyclic AMP response element–binding protein
34 (CREB) signaling. Moreover, SA treatment promoted lipolysis via a PKA/p38-mediated pathway.
35 Our findings may allow us to open a new avenue of strategies against obesity and need further
36 investigation.

37

38 **INTRODUCTION**

39 Brown adipose tissue (BAT) in adult humans was discovered recently in imaging studies and has
40 a function opposite to that of white adipose tissue (1). The unique feature of BAT is expression of
41 UCP1, which helps to dissipate energy by diminishing the proton gradient in the inner membrane
42 of mitochondria (2). Cold exposure of adult human obese and normal subjects has various
43 physiologically beneficial effects such as increased glucose uptake and increased insulin
44 sensitivity (3). In addition, cold exposure has been shown to cause BAT activation (4).

45 Thus, the well-known method for activation of BAT is cold exposure, which increases
46 norepinephrine secretion and thermogenesis. In a study on a mouse model, it has been
47 demonstrated that differentiation of brown fat is accompanied by mitochondrial biogenesis (5).
48 Another study (on a brown preadipocyte cell line) has revealed that BMP7 treatment significantly
49 increases the expression of genes involved in mitochondrial biogenesis and function, including
50 *Pgc-1 α* and *Nrf1* (6).

51 Certainly, PPAR γ is the central regulator of both white fat and brown fat cell development. C/EBP
52 family members function cooperatively with PPAR γ and stimulate a transcriptional cascade to
53 maintain a stable differentiated state of adipocytes. One report suggests that PPAR γ is necessary
54 for brown-fat development but not sufficient to drive the full brown-fat program (which requires
55 additional factors) (7). Other studies offer evidence that transcriptional regulators including
56 PPAR γ , PGC-1 α , PRDM16, and C/EBP β can stimulate the development of brown fat (7, 8).
57 Recently, research revealed that phytochemicals such as rutin activate brown fat, and
58 cryptotanshinone promotes brown-adipocyte commitment among mesenchymal stem cells (9, 10).

59 In rodents, external stimuli lead to activation of β -adrenergic receptor 3 (β -3-AR) by sympathetic
60 stimulation and increased cAMP production, which activates PKA and downstream genes of PKA
61 (11). The activation of PKA promotes the release of fuel (free fatty acids) for thermogenesis. In
62 mice, PKA modulates lipolysis activation involving β 3-AR signaling which increases adenylyl
63 cyclase activity and raises intercellular cAMP concentration (12). The elevated cAMP level
64 triggers PKA, which phosphorylates HSL, ATGL, and perilipin, and thus subsequently initiates
65 lipolysis (13). One report suggests that PKA upregulates UCP1 and plays role in both brown-
66 adipocyte differentiation and mitochondrial biogenesis (11).

67 Sinapic acid (SA) is a natural alkaloidal amine found in black mustard seeds, wine, and vinegar.
68 SA has been reported to have several biological functions, including antioxidant, anti-
69 inflammatory, anticancer, antimicrobial, antimutagenic, and antianxiety activities (14). On the
70 other hand, to date, the effects of SA on thermogenesis remain unexplored. In this study, we used
71 BAT cells to find out the effect of SA on thermogenesis. We propose that SA holds promise as a
72 potential secondary metabolite with a thermogenesis-promoting ability.

73

74 **RESULTS**75 **SA increases the expression of thermogenic markers and promotes mitochondrial biogenesis**
76 **in brown adipocytes**

77 During screening of 854 phytochemicals as described in our previous study (15) to find potential
78 browning-thermogenic compounds, we found that SA can promote the activation of brown
79 adipocytes. To decipher its function, at first, we tested the toxicity of SA toward brown adipocytes
80 at indicated concentrations (Fig. 1A). It turned out that SA is not cytotoxic up to 72h. Here, we
81 compared the effects of SA with those of a well-known thermogenic inducer, Rosi, and BMP7 on
82 the expression of thermogenic signature genes. SA treatment significantly enhanced *Ucp1* mRNA
83 expression, by 1.8-fold (Fig. 1B). Additionally, SA treatment increased the mRNA expression
84 levels of *Prdm16* (1.3-fold) and *Pgc-1 α* (5.4-fold; Fig. 1B). As shown in Fig. 1C, SA treatment
85 raised the protein expression levels of PRDM16, PGC-1 α , PPAR γ , and UCP1. The quantification
86 data revealed that SA treatment increased UCP1 protein expression 1.7-fold, PGC-1 α 1.9-fold,
87 PRDM16 1.5-fold, and PPAR γ protein expression 1.8-fold (Fig. 1C). It has been reported that
88 PPAR γ and PGC1 α activation can promote mitochondrial biogenesis. So, we tested some of the
89 mitochondrial-biogenesis-related genes: *Cox7a*, *Cox8b* and *Nrf1*. As shown in Fig. 2A, SA
90 increased mitochondrial biogenesis related markers. Then, we performed immunostaining with
91 MitoTracker and quantify the stain. As shown in Fig. 2B, SA treated cells showed higher
92 mitochondrial mass than MDI. Next, we measured mtDNA expression and found that SA
93 significantly increased mtDNA (Fig. 2C). After that, we needed to test whether mitochondrial
94 biogenesis leads to increased oxygen consumption. As shown in Fig. 2D, SA treatment increased
95 oxygen consumption. These data enabled us to propose that SA can induce the expression of
96 thermogenic and mitochondrial biogenesis markers.

97 SA activates the PKA pathway in brown adipocytes

98 Of note, we found that SA and H89 share the ATP-binding pockets on the PKA surface via both
99 hydrogen and hydrophobic interactions (Fig. 3A). SA and H89 seem to share amino acid residues
100 Phe³²⁷, Glu⁹¹, Ala⁷⁰, Lys⁷², Thr¹⁸³, Leu¹⁷³, Val⁵⁷, and Asp¹⁸⁴ in the active site of PKA (Fig. 3A).
101 Structural analysis revealed that the binding-affinity values of SA and H89 are -6.2 and -8.3
102 kcal/mol, respectively, implying that H89 binds more strongly than SA, but SA has the ability to
103 slightly inhibit the activity of H89, as confirmed by western blotting (Fig. 3B). We increased the
104 SA concentration and treated PKA with H89; we found that SA treatment inhibited the H89
105 activity (Fig. 3B). The molecular docking analysis suggests that SA may be a potent agonist for
106 induction of PKA phosphorylation.

107 On the basis of this finding, we investigated PKA signaling during SA treatment. We found that
108 SA treatment increases PKA substrate phosphorylation at 60 min as compared to the MDI medium
109 (Fig. 3C). We also tested the phosphorylation of other downstream kinases of PKA signaling,
110 where we found that SA stimulates phosphorylation of CREB, p38, and ERK as well (Fig. 3D).
111 We also observed that SA treatment promoted phosphorylation of HSL (Ser⁵⁶³ and Ser⁶⁶⁰) on day
112 6 during brown-adipocyte differentiation (Fig. 3E). In addition, we assessed triglyceride (TG)
113 accumulation by ORO staining (Supplemental Fig. 1A and B).

114 To understand the function of SA in thermogenic gene induction, we confirmed the expression of
115 PKA downstream genes, *Ucp1*, *Pgc1 α* and *Prdm16* in SA treated condition along with an activator
116 of cAMP-dependent protein kinase, 8-bromoadenosine 3'.5'-cyclicmophosphate (8-Br-cAMP)
117 (Fig. 4A and 4B). Data suggested SA can effectively induce thermogenic genes. To confirm PKA
118 signaling in SA-treated brown adipocytes, we tried to assess the effect of PKA inhibition on SA-
119 mediated PKA substrate phosphorylation (Fig. 4C and 4D). The expression of downstream

120 thermogenic target genes of PKA, e.g., *Ucp1*, *Pgc1 α* , *Ppar γ* , and *Cebpa* was diminished by H89
121 treatment, but this effect was reversed by cotreatment with SA (Fig. 4C). As depicted in Fig. 4D,
122 HSL (Ser⁵⁶³ and Ser⁶⁶⁰) and CREB (Ser¹³³) phosphorylation was dramatically inhibited during H89
123 treatment. By contrast, during cotreatment with SA, the phosphorylation was significantly
124 recovered.

125 We next studied the activities of the PKA signaling pathway during *PKA-cat- α* gene silencing
126 and SA treatment (Fig. 4E). As illustrated in Fig. 4E, *PKA-cat- α* siRNA inhibited the mRNA
127 expression of *PKA-cat- α* effectively. As expected, the expression of the downstream genes in the
128 PKA signaling pathway was reduced by *PKA-cat- α* gene silencing, but this effect was attenuated
129 by SA treatment (Fig. 4F and 4G). Overall, we can propose that SA contributes to brown-adipocyte
130 activation and lipolysis via activation of PKA signaling (Fig. 4H).

131

132 **DISCUSSION**

133 Stimulation of brown adipocytes and UCP1 mediated heat production require activation of
134 adipocytes and muscle cell surface receptors, such as Trpv1, β -3-AR, Ptch1, A2aR and TrkB. These
135 receptors require cellular signaling cascades such as PKA, PKG, Sirt1, AMPK, and p38 MAPK,
136 cytokines (IL-4 and IL-13), and transcriptional regulators, such as Prdm family, Pgc-1 α , Ppar
137 family, and Zfp516 for UCP1 expression (16).

138 Several plant-extracted compounds (berberine, butein, capsaicin, and fucoxanthin), artificially
139 synthesized compounds (e.g., a Ppar γ agonist, β -3-AR agonist, and salsalate), and endogenous
140 small-molecule factors (e.g., serotonin, lactate, and adenosine) have been identified as potential
141 BAT activators that turn on thermogenic transcriptional factors by involving their cell surface
142 receptors or by cellular signaling cascades modulation (16). Our data revealed that SA acts as a
143 potent stimulator of brown-adipocyte activation. The protein factors that control brown-fat
144 differentiation were upregulated by SA treatment, including PPAR γ , PGC-1 α , CEBP β , and
145 PRDM16 along with increased expression of UCP1. mRNA and protein expression levels of a key
146 thermogenic marker, UCP1, were increased by SA treatment here, indicating activation of mature
147 BAT adipocytes. HSL activity appears to be regulated by site-specific phosphorylation on at least
148 five serine residues (Ser⁵⁶³, Ser⁵⁶⁵, Ser⁶⁰⁰, Ser⁶⁵⁹, and Ser⁶⁶⁰), and PKA phosphorylates HSL at
149 Ser⁵⁶³, Ser⁶⁵⁹, and Ser⁶⁶⁰ (17, 18). SA increases the phosphorylation of HSL (Ser⁵⁶³ and Ser⁶⁶⁰);
150 during browning and during thermogenic activation of BAT, similar changes with increased
151 lipolysis have been observed (19).

152 The differentiation and physiological functions of brown adipocytes are closely related to enhance
153 mitochondrial biogenesis. Researcher has demonstrated that PPAR γ and transcriptional

154 coactivator PGC-1 α can contribute to mitochondrial function and biogenesis (20) which are
155 similar to our findings although further investigation is needed for molecular mechanism.

156 Computational identification of PKA agonist has been described elsewhere (21) where, lead
157 compound share same binding site as SA, but described as an agonist of PKA. H89 inhibits the
158 activation of CREB and the CREB-mediated MKP-1 induction by lipopolysaccharide (LPS)
159 resulting from the inhibition of PKA and MSK by H89 (22). Protein kinases catalyzes the transfer
160 of γ -phosphate of ATP to the hydroxyl group present in a tyrosine, serine, or threonine residue to
161 phosphorylate their substrates. The direct effects of H89 on active site of the enzyme causes its
162 inhibitory actions. It also looked likely that H89 obstructs protein kinase activity via interacting
163 with the free enzyme, not with the enzyme-ATP complex (23). PKA mediates forskolin-induced
164 CREB phosphorylation through p38 and MSK1 in NIH 3T3 cells (24). In our study, H89 treatment
165 inhibited PKA phosphorylation resulting lower effect of SA on HSL phosphorylation at PKA
166 target sites, Ser⁵⁶³ and Ser⁶⁶⁰; our data are in agreement with the findings of other researchers (25).

167 SA and H89 both can bind competitively to PKA by sharing the ATP-binding site on a PKA
168 catalytic subunit, as we showed by our molecular docking analysis and confirmed by western
169 blotting. Our data indicate that the expression of target genes of PKA, e.g., *Ucp1*, *Pgc1 α* , *Ppar γ* ,
170 and *Cebp β* , was reduced by H89 treatment, but this suppression was reversed by SA treatment.

171 Besides, SA promoted phosphorylation of CREB, p38, and ERK; CREB phosphorylation was
172 inhibited by H89 treatment, and this change was attenuated by SA treatment. In this context, we
173 propose that SA-mediated PKA activation can induce both phosphorylation of its downstream
174 targets and expression of browning-related genes although a fine-tuned study is needed to confirm
175 this crosstalk.

176 In conclusion, this study revealed that SA not only activates the thermogenic program but also
177 induces lipolysis. SA-mediated thermogenic-signature upregulation is probably involved in the
178 activation of UCP1 via PKA/CREB signaling. Our findings may open up a new avenue of research
179 on the downstream thermogenic program in *in vivo* models.

180

181 MATERIALS AND METHODS

182 Chemicals, reagents, and antibodies

183 SA (purity $\geq 98.0\%$), insulin, dexamethasone, 3-isobutyl-1-methylxanthine (IBMX), rosiglitazone
184 (Rosi), 8-bromoadenosine 3'.5'-cyclicmophosphate (8-Br-cAMP), Oil Red O dye (ORO), and
185 3-(4,5-dimethylthiazol-2-yl)-2,5-diphenyltetrazolium bromide (MTT) were purchased from
186 Sigma-Aldrich (St. Louis, MO, USA), and human recombinant BMP7 from R & D Systems
187 (Minneapolis, MN, USA). Fetal bovine serum (FBS) and High-glucose Dulbecco's modified
188 Eagle's medium (DMEM) were bought from Atlas Biologicals (Fort Collins, CO, USA), and a
189 penicillin-streptomycin solution from Hyclone Laboratories, Inc. (South Logan, NY, USA).
190 Antibodies against UCP1, PGC-1 α , PRDM16, and β -actin were purchased from Abcam
191 (Cambridge, MA, USA), whereas antibodies against phospho-HSL (Ser⁵⁶³ and Ser⁶⁶⁰) and HSL
192 from Cell Signaling Technology (Danvers, MA, USA).

193 Cell maintenance and differentiation

194 BAT cells were cultured and maintained in the DMEM GlutaMax medium supplemented with 10%
195 of FBS and 1% of the penicillin-streptomycin solution and were kept at 37°C in a 5% CO₂
196 incubator. BAT cells are an immortalized cell line created by one scientist (26). The cells were
197 differentiated as described elsewhere (27). Cells after 6 days of differentiation were used in all the
198 experiments unless stated otherwise.

199 Cell treatment procedures

200 Fully confluent BAT cells were treated with the MDI differentiation induction medium consisting
201 of 0.5 mM 3-isobutyl-1-methylxanthine, 1 μ M dexamethasone, and 10 μ g/mL insulin in DMEM

202 supplemented with 10% of FBS, followed by a maturation medium composed of DMEM, 10% of
203 FBS, and 10 µg/mL insulin. The media were refreshed every other day. The following treatment
204 groups were set up: MDI, Rosi with MDI (positive control), BMP7 with MDI (positive control),
205 and SA with MDI. Treatments exceeding 2 days were continued until day 4 by mixing drugs with
206 the maturation medium. After day 4, only the maturation medium was used until cell harvesting.
207 Preadipocytes were maintained only in the culture medium (DMEM and 10% of FBS).

208 **Cell viability assay**

209 In 96-well plates, BAT cells were seeded at 80% to 90% confluence. Cell viability was evaluated
210 by MTT assay as described elsewhere (15).

211 **Analysis of mitochondrial DNA content**

212 Mitochondrial biogenesis was quantified by real-time qPCR as described elsewhere (28) assuming
213 that the ratio of mitochondrial DNA (mtDNA) to nuclear DNA (nDNA) increases but nDNA
214 remains constant.

215 **Oxygen consumption assay**

216 BAT cells were seeded in a 96-well plate at a density of approximately 40,000-60,000 cells per
217 well. Oxygen consumption assay was performed as kit protocol (Cayman, Ann Arbor, MI, USA).

218 **Quantitative reverse-transcription PCR (qRT-PCR) analyses**

219 Total-RNA extraction from (and qRT-PCR analyses of) BAT cells were performed as described
220 previously (29). The primer sequences employed in this study are listed in Supplemental Table 1.
221 Expression of target genes was normalized to that of TATA box-binding protein (*Tbp*).

222 Preparation of whole-cell extracts for western blot (WB) analyses

223 Whole-cell extracts from BAT cells were prepared as described elsewhere (30) with a minor
224 modification. Briefly, cell extracts were collected after 6 days of differentiation. Next, 1% BSA
225 was used for blocking the membranes instead of skim milk (because of analysis of
226 phosphoproteins), and a phosphatase inhibitor cocktail (Sigma-Aldrich) was added into RIPA lysis
227 buffer (Santa Cruz Biotechnology, Inc.).

228 Gene silencing experiments

229 Gene silencing assay was conducted as described previously (31).

230 *In silico* analysis

231 Western blot analysis revealed that SA upregulates phosphorylation of PKA in the absence of
232 inhibitor H89 and attenuates H89-mediated dephosphorylation. To understand the mechanism
233 better, molecular-docking-based structural analysis was performed. First, crystal structure of
234 cAMP-dependent protein kinase (PDB ID: 1BX6) with a potent inhibitor, balanol (a natural
235 product), bound to its catalytic subunit was obtained from Protein Data Bank (www.rcsb.org).
236 After that, the ligand was removed, and a binding grid of (40 × 40 × 40, 1 Å) size was generated
237 containing all possible active sites on PKA surface. Before docking, all the structures were
238 prepared with AutoDock Tools (32), polar hydrogen was added, and finally molecular docking
239 was performed in the AutoDock Vina software (33).

240 Statistics

241 Data are representative of three or more experiments and are shown as mean \pm standard error of
242 the mean (SEM). Student's *t* test was conducted to identify significant changes between a control
243 group and various treatment groups. Data with a P value of < 0.05 were considered statistically
244 significant.

245

246 **ACKNOWLEDGMENTS**

247 This research was supported by the Basic Science Research Program through the National
248 Research Foundation of Korea (NRF) funded by the Ministry of Education
249 (2015R1A6A103032522), and partially by a research fund of Soonchunhyang University.

250

251 **CONFLICTS OF INTEREST**

252 The authors declare that they have no conflicts of interest.

253

1B7CFF97H98.DFCC

254 **FIGURE LEGENDS**

255 **Figure 1.** SA induces expression of *Ucp1* along with other thermogenic genes. (A) Viability of
256 brown adipocytes was assessed by the MTT assay at 24, 48, and 72 hr. Data are expressed as
257 mean \pm SD of three independent experiments. qRT-PCR analysis was performed as described in
258 the *Materials and Methods* section. (B) mRNA expression of brown-fat-specific markers: *Ucp1*,
259 *Pgc-1 α* , and *Prdm16*. Data are presented as mean \pm SEM of three individual experiments. (C)
260 Protein expression levels of brown-fat-specific markers UCP1, PRDM16, PPAR γ , and PGC-1 α .
261 β -actin served as a loading control. Quantification of the protein expression levels of the brown-
262 fat-specific markers. *A significant difference from group MDI (*P < 0.05, **P < 0.01, ***P <
263 0.001).

264 **Figure 2.** SA increases mitochondrial biogenesis. (A) mRNA expression of mitochondrial-
265 biogenesis-related markers: *Cox7a*, *Cox8b*, and *Nrf1*. Data are presented as mean \pm SEM of three
266 individual experiments. (B) MitoTracker immunostaining images of BAT cells. Data are
267 representative of three independent experiments. Quantification of the immunostaining images.
268 Data are expressed as mean \pm SD of three independent experiments. (C) Relative mitochondrial
269 *Cox1* DNA content (ratio of nDNA *p0* and mtDNA *Cox1*). (D) A Luxcel MitoXpress fluorescence
270 assay was conducted to determine the oxygen consumption rate. Gox =glucose oxidase (positive
271 control), AA =antimycin A (negative control). Data are shown as % of control (group MDI) \pm SD
272 from three independent experiments. *A significant difference from group MDI (*P < 0.05, **P <
273 0.01, ***P < 0.001).

274 **Figure 3.** SA activates PKA pathways in BAT cells. (A) Structural analysis of SA and the pan-
275 PKA inhibitor H89 in complex with PKA. They share the same binding pocket on the PKA surface,

276 and the active-site amino acid residues Phe³²⁷, Glu⁹¹, Ala⁷⁰, Lys⁷², Thr¹⁸³, Leu¹⁷³, Val⁵⁷, and Asp¹⁸⁴
277 were found to be common for the interactions of SA and H89 with PKA. (B) Competition between
278 the pan-PKA inhibitor H89 and SA. (C) WB images of phosphorylation levels of PKA substrates
279 during SA (50 μ M) treatment at the indicated time points. (D) Phosphorylation of CREB (Ser¹³³),
280 p38, and ERK during SA (50 μ M) treatment at the indicated time points. (E) WB images of
281 phosphorylation levels of HSL (Ser⁵⁶³ and Ser⁶⁶⁰) under the influence of SA treatment. Rosi:
282 Rosiglitazone, BMP7: bone morphogenic protein 7. β -actin was used as a loading control.

283 **Figure 4.** The function of PKA in SA-mediated differentiation of brown adipocytes. (A-B)
284 Comparison of PKA downstream targets after SA and PKA activator, 8-bromoadenosine 3'.5'-
285 cyclicmophosphate (8-Br-cAMP) treatment. (C-D) The expression of PKA downstream targets
286 after SA (50 μ M) and/or H89 (10 μ M) treatment. (E-F) mRNA expression levels of *PKA-cat-a1*
287 and downstream target genes of PKA, e.g., *Ucp1*, *Pgc-1 α* , *Ppar γ* , and *Cebp α* in BAT cells (6 days
288 of differentiation) after the knockdown of the *PKA-cat-a1* gene. Data are expressed as mean \pm
289 SEM of three independent experiments. *A significant difference from group MDI (*P < 0.05,
290 **P < 0.01, ***P < 0.001). (G) Protein expression of PKA's downstream genes (*Ucp1*, *Ppar γ* ,
291 *Pgc-1 α* , and *Hsl*) and phosphorylation levels of HSL (Ser⁵⁶³ and Ser⁶⁶⁰) in BAT cells (6 days of
292 differentiation) after the knockdown of the *PKA-cat-a1* gene. (H) A schematic model of SA-
293 mediated lipolysis and differentiation of brown adipocytes via the PKA pathway.

294

295 REFERENCES

- 296 1. Vijgen GH, Sparks LM, Bouvy ND et al (2013) Increased oxygen consumption in human
297 adipose tissue from the “brown adipose tissue” region. *J Clin Endocrinol Metab* 98, E1230-
298 E1234
- 299 2. Nedergaard J, Golozoubova V, Matthias A, Asadi A, Jacobsson A and Cannon B (2001)
300 UCP1: the only protein able to mediate adaptive non-shivering thermogenesis and
301 metabolic inefficiency. *Biochim Biophys Acta Bioenerg* 1504, 82-106
- 302 3. Chondronikola M, Volpi E, Børsheim E et al (2014) Brown adipose tissue improves whole-
303 body glucose homeostasis and insulin sensitivity in humans. *Diabetes* 63, 4089-4099
- 304 4. Saito M, Yoneshiro T and Matsushita M (2016) Activation and recruitment of brown
305 adipose tissue by cold exposure and food ingredients in humans. *Best Pract Res Clin*
306 *Endocrinol Metab* 30, 537-547
- 307 5. Uldry M, Yang W, St-Pierre J, Lin J, Seale P and Spiegelman BM (2006) Complementary
308 action of the PGC-1 coactivators in mitochondrial biogenesis and brown fat differentiation.
309 *Cell Metab* 3, 333-341
- 310 6. Xue R, Wan Y, Zhang S, Zhang Q, Ye H and Li Y (2013) Role of bone morphogenetic
311 protein 4 in the differentiation of brown fat-like adipocytes. *Am J Physiol Endocrinol*
312 *Metab* 306, E363-E372
- 313 7. Kajimura S, Seale P and Spiegelman BM (2010) Transcriptional control of brown fat
314 development. *Cell Metab* 11, 257-262
- 315 8. Seale P, Kajimura S, Yang W et al (2007) Transcriptional control of brown fat
316 determination by PRDM16. *Cell Metab* 6, 38-54

- 317 9. Yuan X, Wei G, You Y et al (2016) Rutin ameliorates obesity through brown fat activation.
318 FASEB J 31, 333-345
- 319 10. Imran KM, Rahman N, Yoon D, Jeon M, Lee B-T and Kim Y-S (2017) Cryptotanshinone
320 promotes commitment to the brown adipocyte lineage and mitochondrial biogenesis in
321 C3H10T1/2 mesenchymal stem cells via AMPK and p38-MAPK signaling. *Biochim.*
322 *Biophys. Acta, Mol. Cell. Biol. Lipids* 1862, 1110-1120
- 323 11. Sell H, Deshaies Y and Richard D (2004) The brown adipocyte: update on its metabolic
324 role. *Int J Biochem Cell Biol* 36, 2098-2104
- 325 12. Duncan RE, Ahmadian M, Jaworski K, Sarkadi-Nagy E and Sul HS (2007) Regulation of
326 lipolysis in adipocytes. *Annu Rev Nutr* 27, 79-101
- 327 13. Zimmermann R, Lass A, Haemmerle G and Zechner R (2009) Fate of fat: the role of
328 adipose triglyceride lipase in lipolysis. *Biochim Biophys Acta Mol Cell Biol Lipids* 1791,
329 494-500
- 330 14. Nićiforović N and Abramović H (2014) Sinapic acid and its derivatives: natural sources
331 and bioactivity. *Compr Rev Food Sci Food Saf* 13, 34-51
- 332 15. Imran KM, Yoon D, Lee T-J and Kim Y-S (2018) Medicarpin induces lipolysis via
333 activation of Protein Kinase A in brown adipocytes. *BMB Rep* 51, 249-254
- 334 16. Song N-J, Chang S-H, Li DY, Villanueva CJ and Park KW (2017) Induction of
335 thermogenic adipocytes: molecular targets and thermogenic small molecules. *Exp Mol*
336 *Med* 49, e353
- 337 17. Watt MJ, Holmes AG, Pinnamaneni SK et al (2006) Regulation of HSL serine
338 phosphorylation in skeletal muscle and adipose tissue. *Am J Physiol Endocrinol Metab* 290,
339 E500-E508

- 340 18. Anthonsen MW, Rönstrand L, Wernstedt C, Degerman E and Holm C (1998)
341 Identification of novel phosphorylation sites in hormone-sensitive lipase that are
342 phosphorylated in response to isoproterenol and govern activation properties in vitro. *J Biol*
343 *Chem* 273, 215-221
- 344 19. Barneda D, Frontini A, Cinti S and Christian M (2013) Dynamic changes in lipid droplet-
345 associated proteins in the “browning” of white adipose tissues. *Biochim Biophys Acta Mol*
346 *Cell Biol Lipids* 1831, 924-933
- 347 20. Corona JC and Duchon MR (2015) PPAR γ and PGC-1 α as therapeutic targets in
348 Parkinson's. *Neurochem Res* 40, 308-316
- 349 21. Natarajan P, Swargam S, Hema K, Vengamma B and Umamaheswari A (2015) E-
350 pharmacophore based virtual screening to identify agonist for PKA-C α . *Biochemistry and*
351 *Analytical Biochemistry* 4, 2161-1009
- 352 22. Cho IJ, Woo NR, Shin IC and Kim SG (2009) H89, an inhibitor of PKA and MSK, inhibits
353 cyclic-AMP response element binding protein-mediated MAPK phosphatase-1 induction
354 by lipopolysaccharide. *Inflamm Res* 58, 863-872
- 355 23. Lochner A and Moolman J (2006) The many faces of H89: a review. *Cardiovasc Drug Rev*
356 24, 261-274
- 357 24. Delghandi MP, Johannessen M and Moens U (2005) The cAMP signalling pathway
358 activates CREB through PKA, p38 and MSK1 in NIH 3T3 cells. *Cell Signal* 17, 1343-1351
- 359 25. Watt MJ and Cheng Y (2017) Triglyceride metabolism in exercising muscle. *Biochim*
360 *Biophys Acta Mol Cell Biol Lipids* 1862, 1250-1259
- 361 26. Park JH, Kang HJ, Kang SI et al (2013) A multifunctional protein, EWS, is essential for
362 early brown fat lineage determination. *Dev Cell* 26, 393-404

- 363 27. Rosenwald M, Perdikari A, Weber E and Wolfrum C (2013) Phenotypic analysis of BAT
364 versus WAT differentiation. *Curr Protoc Mouse Biol* 3, 205-216
- 365 28. Schild L, Dombrowski F, Lendeckel U, Schulz C, Gardemann A and Keilhoff G (2008)
366 Impairment of endothelial nitric oxide synthase causes abnormal fat and glycogen
367 deposition in liver. *Biochim Biophys Acta Mol Basis Dis* 1782, 180-187
- 368 29. Rahman N, Jeon M and Kim YS (2016) Delphinidin, a major anthocyanin, inhibits 3T3-
369 L1 pre-adipocyte differentiation through activation of Wnt/ β -catenin signaling. *Biofactors*
370 42, 49-59
- 371 30. Jeon M, Rahman N and Kim Y-S (2016) Wnt/ β -catenin signaling plays a distinct role in
372 methyl gallate-mediated inhibition of adipogenesis. *Biochem Biophys Res Commun* 479,
373 22-27
- 374 31. Yoon D, Imran KM and Kim Y-S (2018) Distinctive effects of licarin A on lipolysis
375 mediated by PKA and on formation of brown adipocytes from C3H10T1/2 mesenchymal
376 stem cells. *Toxicol Appl Pharmacol* 340, 9-20
- 377 32. Morris GM, Huey R, Lindstrom W et al (2009) AutoDock4 and AutoDockTools4:
378 Automated docking with selective receptor flexibility. *J Comput Chem* 30, 2785-2791
- 379 33. Trott O and Olson AJ (2010) AutoDock Vina: improving the speed and accuracy of
380 docking with a new scoring function, efficient optimization, and multithreading. *J Comput*
381 *Chem* 31, 455-461

382

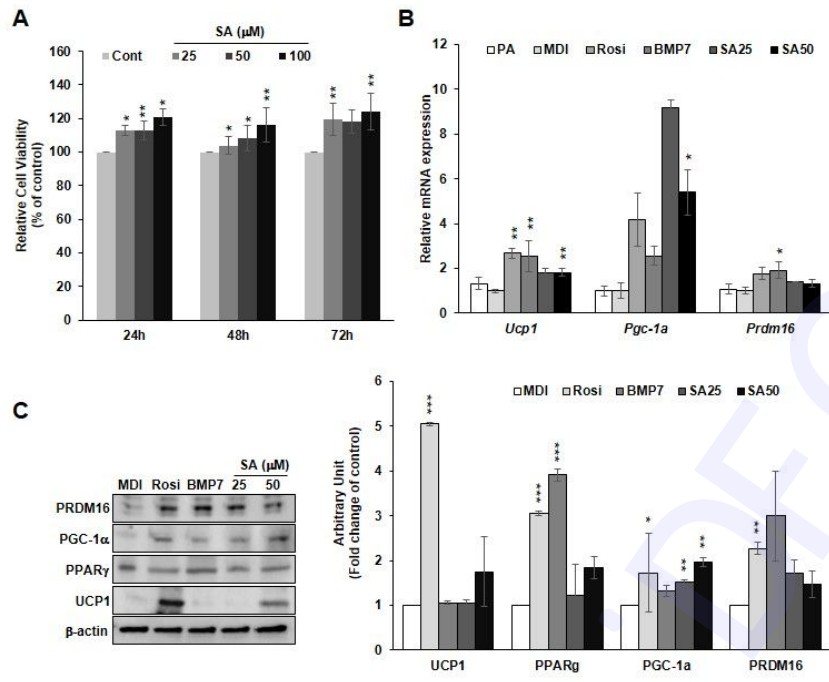


Fig. 1

Fig. 1. Fig. 1

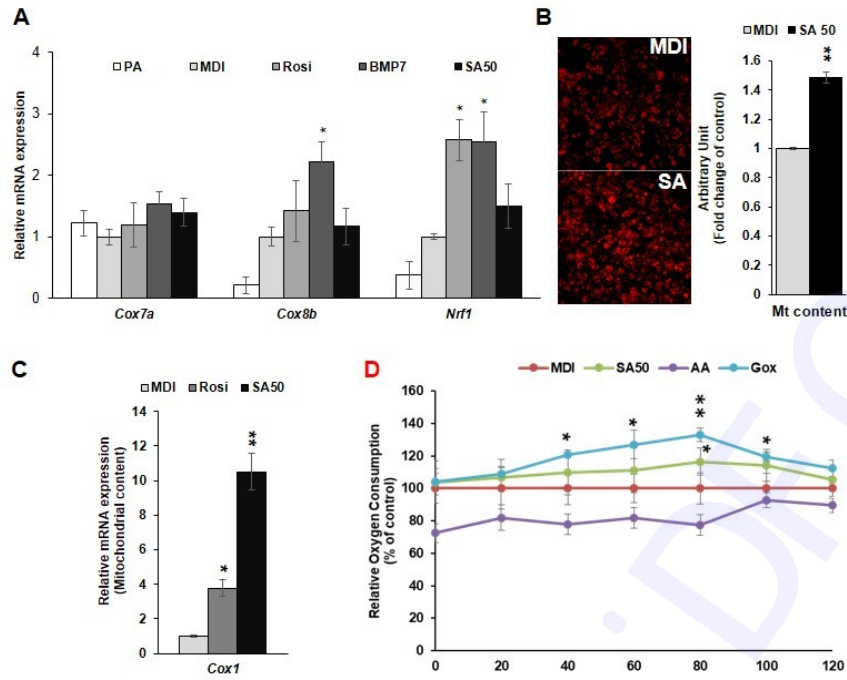


Fig. 2

Fig. 2. Changed Fig. 2

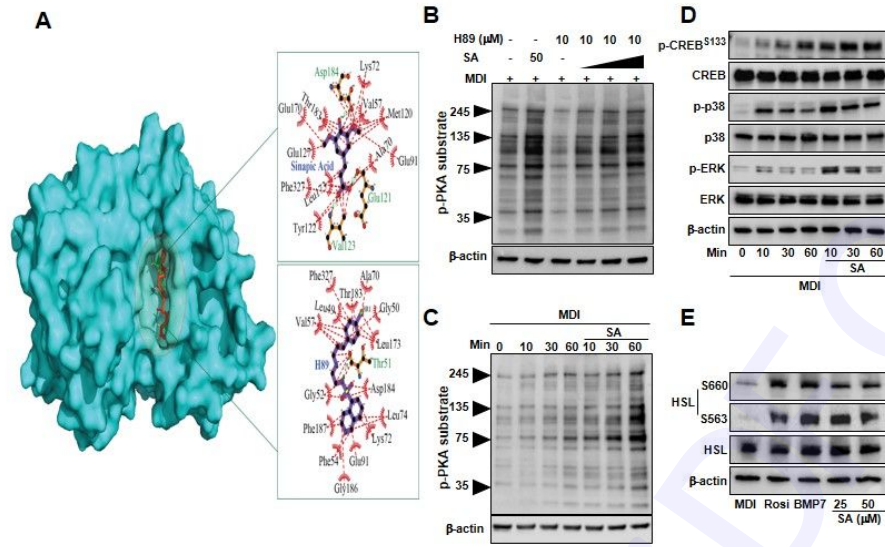


Fig. 3

Fig. 3. Fig. 3

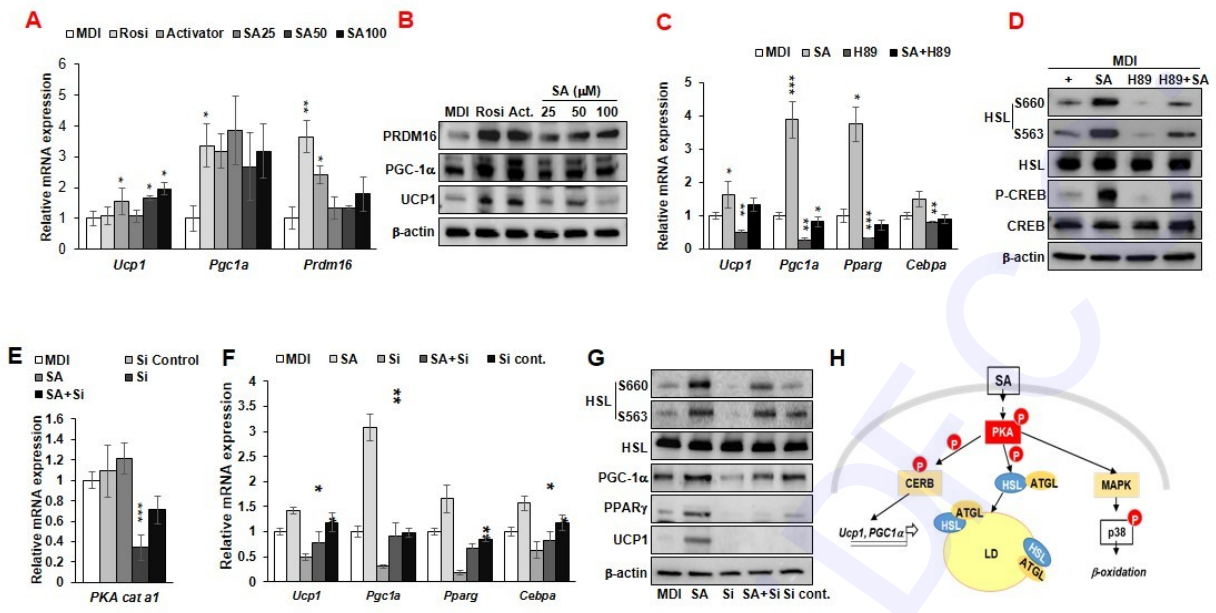
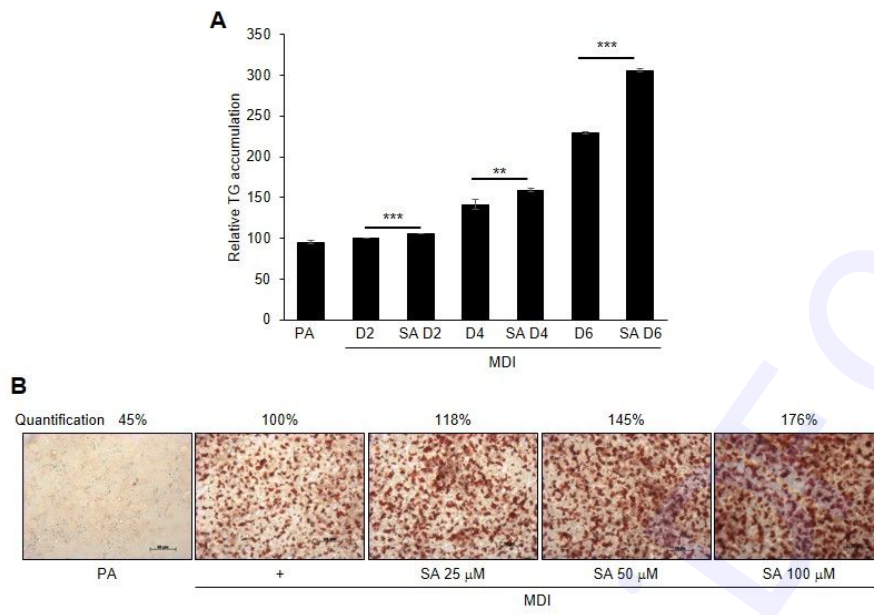


Fig. 4

Fig. 4. changed Fig. 4

Supplemental Table 1. qRT-PCR Primer sets for this study

Name	Primer Sequences (5'-3')	
	Forward	Reverse
<i>Tbp</i>	GAAGCTGCGGTACAATTCCAG	CCCCTTGTACCCTTCACCAAT
<i>Ucp1</i>	GGCATTTCAGAGGCAAATCAGCT	CAATGAACACTGCCACACCTC
<i>Pgclα</i>	AGCCGTGACCACTGACAACGAG	GCTGCATGGTTCTGAGTGCTAAG
<i>Prdm16</i>	CAGCACGGTGAAGCCATTC	GCGTGCATCCGCTTGTG
<i>Cebpa</i>	GAGCCGAGATAAAGCCAAACA	CGGTCATTGTCACTGGTCAACT
<i>Pparγ</i>	TTTGAAAGAAGCGGTGAACCAC	ACCATTGGGTCAGCTCTTGTG
<i>Klf</i>	TGAACGTCTTCCTCCCTGAC	GGTCTGGTGGGAGCTGAATA
<i>aP2</i>	GTGATGCCTTTGTGGGAAACCTGG AAG	TCATAAACTCTTGTGGAAGTCAC GCC
<i>Pref</i>	GGAGAAAGGCCAGTACGAATG	CACAGAAGTTGCCTGAGAAGC
<i>Wnt10a</i>	CCACTCCGACCTGGTCTACTTTG	TGCTGCTCTTATTGCACAGGC
<i>Wnt10b</i>	GCTGACTGACTCGCCCACC	AAGCACACGGTGTTGGCCGT
<i>Cox7a</i>	CAGCGTCATGGTCAGTCTGT	AGAAAACCGTGTGGCAGAGA
<i>Cox8b</i>	GAACCATGAAGCCAACGACT	CGCAAGTTCACAGTCGTTCC
<i>Nrf1</i>	CAACAGGGAAGAAACGGAAA	GCACCACATTCTCCAAAGGT
<i>Cox1</i>	TCTACATTCGGAGCCTGAG	CTACTGATGCTCCTGCATGG



Supplemental Fig. 1

Sup. 2.